

Saturated and Multi-Colored Electroluminescence from Quantum Dots Based Light Emitting Electrochemical Cells

Gang Qian, Ying Lin, Guillaume Wantz, Andrew R. Davis, Kenneth R. Carter, and James J. Watkins*

Novel light emitting electrochemical cells (LECs) are fabricated using CdSe-CdS (core-shell) quantum dots (QDs) of tuned size and emission blended with polyvinylcarbazole (PVK) and the ionic liquid 1-butyl-3-methylimidazolium hexafluorophosphate (BMIM-PF₆). The performances of cells constructed using sequential device layers of indium tin oxide (ITO), poly(3,4-ethylenedioxythiophene)-poly(styrenesulfonate) (PEDOT:PSS), the QD/PVK/IL active layer, and Al are evaluated. Only color saturated electroluminescence from the QDs is observed, without any other emissions from the polymer host or the electrolyte. Blue, green, and red QD-LECs are prepared. The maximum brightness ($\approx 1000 \text{ cd m}^{-2}$) and current efficiency (1.9 cd A^{-1}) are comparable to polymer LECs and multilayer QD-LEDs. White-light QD-LECs with Commission Internationale d'Eclairage (CIE) coordinates (0.33, 0.33) are prepared by tuning the mass ratio of R:G:B QDs in the active layer and voltage applied. Transparent QD-LECs fabricated using transparent silver nanowire (AgNW) composites as the cathode yield an average transmittance greater than 88% over the visible range. Flexible devices are demonstrated by replacing the glass substrates with polyethylene terephthalate (PET).

and stability.^[8] Moreover, a variety of passivated ligands enables the processing of QDs using a range of solvents and facilitates their incorporation into organic matrices including polymers. All of those unique properties make QDs promising materials for low-cost and solution-processed light emitting devices. However, due to the low lying valence band, the use of QDs in light emitting diodes (LEDs) usually requires either blending with organic matrices^[9] or by building a multilayer structure^[3,10,11] to facilitate the charge injection and transport processes that enhance the emission efficiency. Unfortunately, because of the charge-tunneling barrier due to the presence of insulating surface ligands or insufficient Förster energy transfer from the host materials, devices based on blended active layers often exhibit significant host emission.^[3,9] Further, the multilayer devices require precisely controlled layer thickness

1. Introduction

Semiconductor quantum dots (QDs) are attractive luminescent materials for creating light emitting devices because of their size-tunable band gaps, high photoluminescence (PL) quantum yield, good stability and saturated colors with a narrow bandwidth.^[1-7] Emission from QDs can be easily tuned over a wide wavelength range from visible^[1] to near-infrared^[7] just by varying their size rather than their composition. Surface modifications, including the use of core-shell structures, can effectively improve the photoluminescence quantum efficiencies (>50%)

and energy level alignment for each electron and hole transport layer, and are thus limited by complex architectures and voltage-dependent electroluminescence.

Light emitting electrochemical cells (LECs) are alternative but often overlooked light emitting devices that were first invented in 1995.^[12] Compared to LEDs, the main difference is that LECs contain high concentrations of electrolytes in the active layer. When a sufficiently high voltage is applied, the conjugated polymer (in PLECs) is electrochemically oxidized and reduced and forms *p*- and *n*-type doped areas near the anode and cathode, respectively. The incorporated electrolytes are dissociated and redistributed as counter ions to compensate for the corresponding reduced and oxidized species. Owing to the high conductivity of the doped layer between the electrode and light emitting interface, the charge injection barriers are reduced, which enhances the injection of further charges, ultimately leading to the enhancement of emission efficiency regardless of the electrode work function. This model of operation, referred to as the electrochemical doping model (ECD), was proposed by the inventors and supported by some other researchers.^[12-16] In fact, however, the mechanism of operation of LECs is complicated and it is still controversial.^[17-19] Another widely used model for LECs is the electrodynamic model (ED), which suggests that there is no redox reaction in the devices. Rather, the applied voltage only causes the anions and cations

Dr. G. Qian, Dr. Y. Lin, A. R. Davis, Prof. K. R. Carter,
Prof. J. J. Watkins
Department of Polymer Science and Engineering
University of Massachusetts-Amherst
120 Governors Drive
Amherst, MA 01003, United States of America
E-mail: watkins@polysci.umass.edu

Prof. G. Wantz
IMS laboratory
Bordeaux Institute of Technology (IPB)
University of Bordeaux
CNRS UMR 5218, ENSCBP
16 Pey Berland 33607, Pessac Cedex, France



DOI: 10.1002/adfm.201400167

to drift towards the anodes and cathodes, respectively.^[20,21] Recently, a unifying model suggested that either mechanism could be operative, depending on the ability of the device to form non-injection-limited ohmic contacts.^[18] While these two models seem to conflict, either the highly conductive layers or the high electric field between the electrode and the active layer interface will reduce the energy barrier and enhance the carrier injection, which is ideal for the incorporation of QDs using a simple device configuration.

Since the first LEC device was reported almost 20 years ago, most of the related-research has been devoted to devices incorporating conjugated polymers (PLECs)^[12,22–26] and ionic transition-metals complexes (iTMC-LECs).^[27–33] To date, QDs-LECs are still rare. Recently one example was demonstrated by blending CdSe/ZnS core-shell QDs with PF/PPV copolymer, poly [(9,9-dioctyl-2,7-divinylene-fluorenylene)-alt-co-{2-methoxy-5-(2-ethyl-hexyloxy)-1,4-phenylene}], and the polymerizable ionic liquid allyltriethylammonium allylsulfonate (ATOAAS) as electrolytes.^[34] Bright and voltage independent electroluminescence (EL) was obtained and precise color control in a single layer device was achieved. However, due to the blend of the highly emissive conjugated copolymer PF/PPV, the host emission from the copolymer was clearly observed. Our motivation in this study is to make high efficient QDs-LECs without any emissive conjugated polymers, so that devices exhibit only bright and saturated emission from QDs. In our work, QDs with different emissions were blended with the non-conjugated polymer, polyvinylcarbazole (PVK), and the ionic liquid 1-butyl-3-methylimidazolium hexafluorophosphate (BMIM-PF₆) as the electrolyte. The performances of the devices were evaluated using the following device configuration: indium tin oxide (ITO)/ poly(3,4-ethylenedioxythiophene)-poly(styrenesulfonate) (PEDOT:PSS)/ QD active layer/Al. The devices exhibit maximum brightnesses of ≈ 1000 cd m⁻², current efficiencies of (1.9 cd A⁻¹) and power efficiencies of 1.3 lm W⁻¹, which are comparable to the polymer LECs and multilayer QDs-LEDs. By tuning the size of the QDs, blue, green, orange and red QDs-LECs were prepared using the same device structures and procedures. In addition, by utilizing silver nanowire composite as the cathode, transparent QDs-LECs were demonstrated with an average transmittance higher than 88% over the whole visible range. Moreover, by replacing the glass substrate with flexible polyethylene terephthalate (PET) substrate, flexible devices were demonstrated opening an exciting range of potential applications.

2. Results and Discussion

Quantum dots are usually protected by ligands to prevent their aggregation. The nature of ligand strongly affects the solubility,

stability and even the optoelectronic properties of semiconductor QDs. The QDs of different colors and different sizes (Figure S1, Supporting Information) we received from QD Vision Inc. were capped by trioctylphosphine oxide (TOPO) and dispersed in the nonpolar solvent toluene, forming a clear and stable solution with high emission efficiency (Table S1, Supporting Information). Aliphatic ligands with long alkyl chains such as TOPO can serve as electronic insulators and can create an insulating barrier around each QDs that interferes with charge injection and transfer in the devices. Surface modification is required to replace the original ligands with more desirable species through a ligand-exchange process. In this work, 4-mercaptobenzoic (4-MBA) acid was chosen to replace the original TOPO ligand in order to increase the miscibility of QDs with the ionic liquid and enhance the charge injection and mobility.

We choose a generalized ligand-exchange strategy that enables sequential surface modification of QDs without affecting the size and shape.^[35] Firstly, triethylxonium tetrafluoroborate (Et₃OBF₄) was employed to replace the original ligand TOPO, thus stabilizing the QDs with BF₄⁻ in polar media. Secondly, the new ligand (i.e., 4-MBA) was added to the BF₄⁻ capped QDs in excess to replace the BF₄⁻. The distinct advantage of this approach is that the BF₄⁻ capped QDs are readily further functionalized by various ligands via a secondary ligand-exchange reaction. **Figure 1** shows the two ligand exchange processes for red QDs (see the Experimental Section). After the ligand exchange, the QDs were successfully transferred from nonpolar solvent toluene to polar solvent cyclohexanone. The hydrophilic nature of the QDs suggests that the replacement of the original ligands was successful. This was confirmed by FTIR spectroscopy (**Figure 2**). The characteristic C–H stretching vibrations at 2800–3000 cm⁻¹ ascribed to TOPO ligand were almost completely eliminated after surface treatment by Et₃OBF₄, indicating the original organic ligand were stripped off. In addition, an intense peak at 1084 cm⁻¹ emerged, which was assigned to the BF₄⁻ anions.^[36] After the second ligand exchange, several new absorption peaks emerged, especially at 1675 and 2559 cm⁻¹, which are assigned to –COOH and –SH, respectively. The TEM images confirmed that the shape and size of the original QDs after ligand exchange were retained (Figure S2, Supporting Information).

The optical properties of QDs with different colors before and after ligand exchange were studied by UV-vis absorption and PL spectroscopy. The results are summarized in Table S1 and the spectra are shown in Figure S3, Supporting Information. Four kinds of QDs with different colors were used in this work: red, orange, green and blue. Their emission peaks are centered at 613 nm, 587 nm, 509 nm, and 444 nm, respectively.

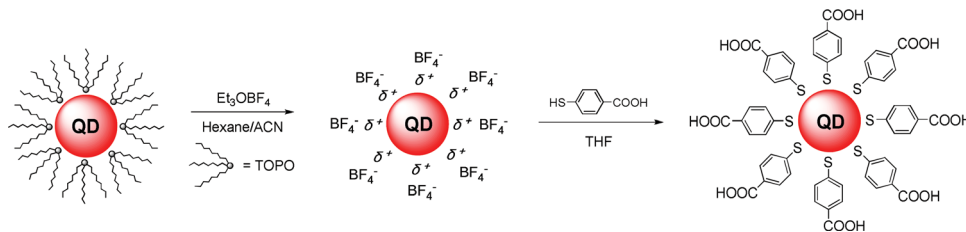


Figure 1. Schematic illustration of the ligand exchange process.

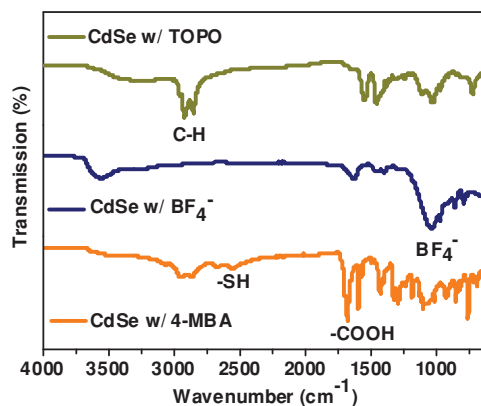


Figure 2. FTIR spectra of red QDs with different ligands.

After ligand exchange, all the absorption and PL spectra profiles are nearly the same. Unlike the spectra profiles, the fluorescence emission quantum yields (Φ_f) decrease significantly. For example, orange QDs capped with TOPO have emission efficiencies as high as 100% (Table S1, Supporting Information), but only around 1/3 of this efficiency (36%) is retained after ligand exchange by 4-MBA. This is likely due to the hole trapping by the thiol.^[37,38] As a consequence, there is a trade-off for QDs between high miscibility with electrolytes and high emission efficiency. As expected, all emission spectra are very narrow, with the full width at half-maximum (FWHM) in range of 21–35 nm, indicating the high color purity and narrow size distribution, making modified QDs promising for use in light emitting devices.

The electroluminescence properties of the QDs were evaluated using light emitting electrochemical cell devices of the following device configuration: ITO/ PEDOT:PSS/QD active layer/Al

(Figure 3a). The results are summarized in Table 1. The active layer containing PVK, QDs and ionic liquid BMIM-PF₆ with mass ratio of 7.5:6:1.5 was deposited by spin coating of the mixture solution from cyclohexanone at speed of 1000 rpm, yielding a layer thickness of approximately 150–200 nm. PVK was chosen as the host polymer to achieve high quality films and for its bandgap to minimize its light emission. In addition, PVK has been demonstrated to enhance photoconductivity of CdS QDs.^[39] Numerous studies on organic LEDs have used PVK as hole transport species.^[40] BMIM-PF₆ was used as electrolytes in LECs devices to redistribute and compensate the doped species. Moreover, BMIM-PF₆ can be mixed with PVK to yield a uniform film upon evaporation. Figure 3b shows the normalized PL and EL spectra of four QD-LECs devices. Highly saturated electroluminescence with Commission Internationale d’Eclairage (CIE) coordinates of (0.67, 0.33), (0.59, 0.38), (0.18, 0.65), and (0.16, 0.06) for red, orange, green and blue QD-LECs, respectively, are obtained. In the whole visible region, only emission from the QDs was observed, without any other emissions from host polymer or ionic liquid. Compared to the corresponding PL spectra in solution, the EL spectra are slightly red shifted (5–10 nm), as previously reported for QD-LEDs.^[41] This attributed to a combination of inter-dot interactions^[42] and electric-field-induced Stark effects.^[43] The FWHM of the QDs emission peaks in the PL and EL are very similar (Table 1 and Table S1, Supporting Information), just 2–3 nm broader for EL spectra, indicating that the high color purity of the QDs is maintained in the LECs. EL spectra at varying voltages were taken to study the voltage dependence of the QD-LECs. Figure 3c shows representative EL spectra for red QD-LECs taken at 6, 8, 10, 12, 14, and 16 V. All of those spectra are nearly the same, which suggests that device color is not significantly affected by the operating voltage, indicating high color stability. All four

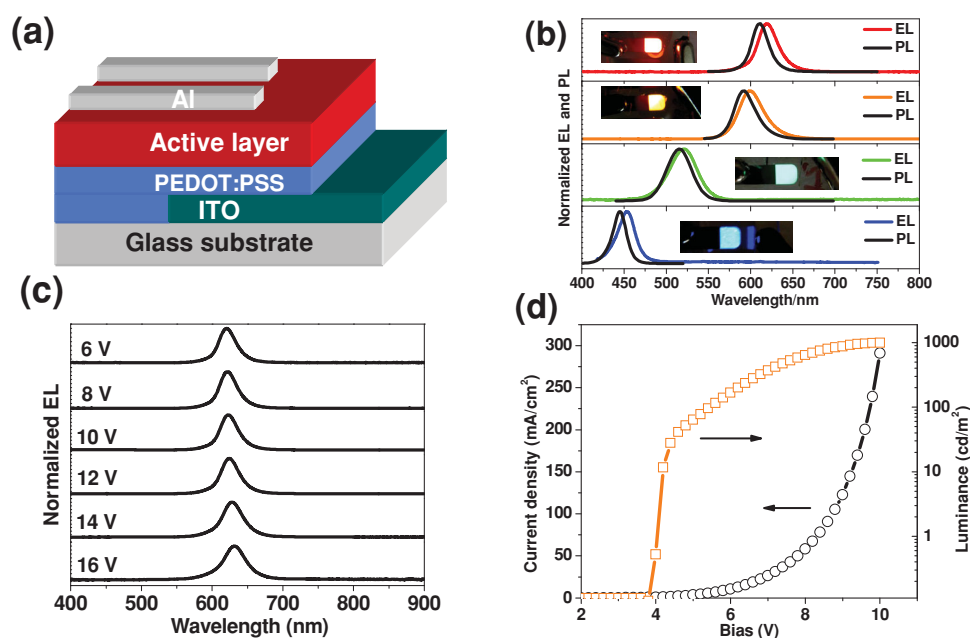


Figure 3. a) Device structure employed in this work. b) Normalized emission spectra of solution photoluminescence and QD-LECs electroluminescence. Inset: photograph of a typical device (pixel size, 6 mm²). c) Normalized EL spectra of red QD-LECs at varying voltages. d) Representative current density–voltage–luminance curves of the QD-LECs.

Table 1. Device performance of QD-LECs.

QDs	V_{on} [V]	λ_{EL} [nm]	L [$\text{cd m}^{-2\text{a}}$]	Current efficiency [cd A^{-1}]	Power efficiency [lm W^{-1}]	FWHM [nm]	CIE
Red	2.0	620	581	1.5	1.0	27	0.67, 0.33
Orange	3.8	600	995	1.9	1.3	34	0.59, 0.38
Green	3.8	520	208	1.2	0.6	39	0.18, 0.65
Blue	4.0	453	18	0.4	0.6	25	0.16, 0.06

V_{on} : turn on voltage [at a luminance (L) of $> 1 \text{ cd m}^{-2}$]; FWHM: full width at half maximum; CIE: Commission Internationale d'Éclairage; ^a L : Luminance, measured at 10 V.

colors of the QD-LECs show voltage-independent EL spectra (Figure S4, Supporting Information).

Figure 3d displays representative current density–voltage (J – V) and luminescence–voltage (L – V) curves of the orange QD-LECs. Before testing, each device was charged to allow the redistribution of the electrolytes and to form the highly conductive layer near the electrode and active layer interface, which facilitates charge injection. Before collecting the current and luminance data, devices were held at 4 V at room temperature for approximately 3 min, until a stable current was reached (Figure S5, Supporting Information). Then the J – V and L – V curves were taken simultaneously by sweeping voltage from 0 to 10 V in 0.2 V increments quickly (≈ 5 s). The devices show a diode like J – V curve, because in over such small time scale, the devices can be considered as fixed-junction LECs with limited relaxation. The devices are also functioning like LEDs with very short turn-on times (turn on instantly) and emission intensities that increase slowly to their maxima in about 4 min. The initial increase of the EL intensity can be associated to the growth of the p - and n -type doped regions (Figure S6, Supporting Information). The device performance gradually degraded after about 5 min and the emission intensity retained 80% of its maximum after one half hour. The brightness of the orange LECs is around 1000 cd m^{-2} at 10 V, which was higher than that of similar QD-LEC employing an emissive conjugated polymer.^[34] The maximum current efficiency and power efficiency were 1.9 cd A^{-1} and 1.3 lm W^{-1} , respectively. These results are comparable to the precisely controlled multilayer LED devices.^[3] The turn on voltage was as low as 2.0 V for red QDs device, which is typical for LEC devices employing ionic liquid as electrolytes. In order to study the role of ionic liquid in the LEC devices, a control device “QD-LED” was made with exactly the same device structure and same experimental procedure based on the red QDs with same mass ratio between QD and PVK, but without ionic liquid in the active layer (Figure S7, Supporting Information). Compared to the corresponding LEC device, the current density for LED was much lower, rendering the LED device non-functional even at high applied voltages. This is due to the large hole injection barrier arising from the large difference between the work function of PEDOT:PSS (≈ 5.0 eV) and the HOMO level of the red QDs (≈ 6.8 eV). The results confirm that the ionic liquid effectively reduces the injection barrier and enhances the efficiency of devices. The performances of the other QD-LECs with different colors are summarized in Table 1. Figures S8–S11 (Supporting Information) show typical current density–voltage, luminance–voltage, current efficiency–current density, and power efficiency–luminance curves. The low turn-on voltages of 2–4 V are typical for LECs and confirm

the reduced energy barrier for charge injection. The low efficiency of blue QD-LECs could be attributed to its low PL yield (Table S1, Supporting Information) and inefficient and incomplete energy transfer from PVK to blue QDs because of its weak absorption across the PVK emission spectrum.

White-light emitting devices are of interest due to their potential applications in the lighting and backlighting in displays. White-light QD-LEDs have been demonstrated by using a mixture of three types of QDs as blue, green and red emitters, respectively.^[44,45] Here the first white-light QD-LEC is demonstrated by blending the different colors of QDs with PVK and ionic liquid, using the same device structure as the monochrome devices. In order to obtain white EL, the mass ratio of R:G:B QDs was varied, taking into account the emission efficiency and energy transfer from higher energy to lower energy QDs.^[46,47] Multiple mass ratios for R:G:B QDs were tested and the optimized ratio to achieve white is 1:16:7 (Table S2, Supporting Information). Because of the low emission efficiency, the green QD has the highest concentration in the blended film.

The EL spectrum of the white QD-LEC with the optimized ratio at 10 V is shown in Figure 4b. Three isolated peaks at wavelengths of 452, 519, and 622 nm are attributed to the blue, green, and red light emitting quantum dots, respectively, in agreement with the EL spectra of the corresponding monochrome QD-LECs devices (Figure 4a). The CIE coordinates of the devices are plotted on the CIE chromaticity diagram in Figure 4c, which includes a photograph of the device operating at 10 V with CIE coordinates (0.33, 0.33). Because it is more difficult to inject holes into the valence band of blue QDs, the relative emission intensity of blue QDs increases at higher voltages (Figure S12, Supporting Information), leading to the white device CIE shifted to the blue. Figure S13 (Supporting Information) displays the current density–voltage (J – V) and luminescence–voltage (L – V) curves of the white QD-LECs. The brightness at 10 V is higher than 100 cd m^{-2} at 200 mA cm^{-2} , and the turn on voltage is 4 V. The maximum luminescence current efficiency is 0.39 cd/A .

Transparent light emitting devices are an interesting research area because of their unique potential applications, including transparent displays for helmet-mounted, windscreen-mounted or other “heads-up” applications.^[48] Several transparent devices have been demonstrated in the past 20 years, including transparent LEDs^[48–50] and LECs.^[51] In practical applications, the main challenge to make highly efficient transparent light emitting devices lies in the transparency of the electrode materials. ITO is the most popular electrode because of its transparency and high conductivity. However, due to the low lying of the work

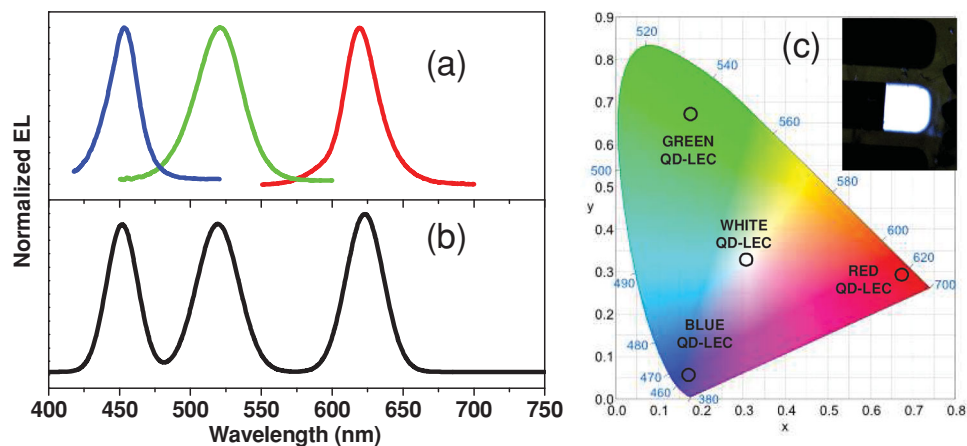


Figure 4. a) Normalized EL spectra of blue, green and red monochrome QD-LECs (blue, green, and red lines, respectively). b) EL spectrum for the white QD-LEC (@ 10 V). c) CIE chromaticity diagram indicating the color of blue, green, red, and white QD-LECs. Inset: photograph of a white QD-LEC in operation with 10 V of applied forward bias with CIE (0.33, 0.33).

function, which will inhibit the electron injection, the use of ITO as cathode is limited. It is also challenging to deposit high quality ITO layers on top of organic coatings. Recently, several candidates for transparent conductors have emerged, including carbon nanotubes,^[52] graphene,^[53] metal grids,^[54] thin metal films,^[55] and silver nanowires (AgNW).^[56,57] In our case, AgNW was used as cathode because of its high optical transparency, high conductivity and solution processability. There are several advantages to the LEC configuration described for transparent devices. These include a simple single layer device structure and the use of optical transparent PVK and ionic liquids in the active layer. Further, the performance of LECs is not highly dependent on the work function of the cathode, which offers freedom of choice for the transparent cathode.

We fabricated red transparent QD-LECs using AgNW composites as the cathode. (see the Experimental Section for details.) **Figure 5a** shows the transmittance spectra of the transparent QD-LECs. The average transmittance in the visible region over 400 nm to 750 nm is 88%. The inset of **Figure 5a** shows a photograph of a highly transparent QD-LEC. The UMass logo located behind the device can be clearly seen. **Figure 5b** shows

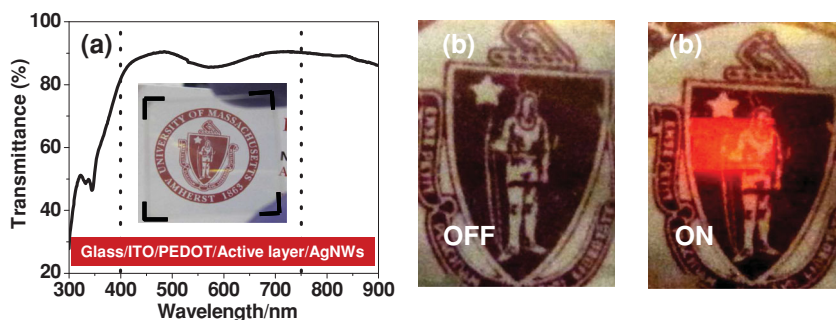


Figure 5. a) Transmission spectrum of the red transparent QD-LECs. The average transmittance in the visible region over 400 nm to 750 nm is 88%. The inset photography shows the transparent QD-LECs. The black brackets indicate the border of the device. b) Photograph of the transparent QD-LECs in on and off states, demonstrating the uniformity of pixel illumination and device transparency.

a photograph of the device in its on and off states. There is high transparency in the off state, while the on state demonstrates uniformity of pixel illumination as well as device transparency.

Flexible light emitting devices are of interest for roll-able displays and electronic paper. In addition, flexible devices can be fabricated by using low-cost and scalable roll-to-roll processes. In this work, by replacing glass substrate with polyethylene terephthalate (PET), flexible QD-LECs were fabricated using either evaporated Al or spin-coated AgNW as the cathode (**Figure S14**, Supporting Information). The performance of devices with Al is comparable to those devices on glass substrate.

3. Conclusions

In conclusion, by adding ionic liquid as an electrolyte in the active layer, QD-LEDs were effectively converted to QD-LECs. The performances of the simple QD-LEC device structures were comparable to precisely controlled multilayer LED devices that require electron or hole injection and transport layers. Saturated and multicolored QD-LECs were fabricated, and the

EL spectra were voltage-independent. Moreover, perfect white-light emission with CIE (0.33, 0.33) was achieved by finely tuning the mass ratio of R:G:B QDs in the LECs and the voltage applied. Transparent and flexible devices were demonstrated by using a silver nanowire composite electrode and a PET substrate.

4. Experimental Section

Materials: All chemicals and reagents were used as received from commercial sources without purification. Quantum dots with different colors were obtained from QD Vision Inc. (Lexington, MA, USA). Poly (9-vinylcarbazole) ($M_w \approx 90\,000$), 1-butyl-3-methylimidazolium hexafluorophosphate,

indium tin oxide nanoparticles dispersion (<100 nm, 30 wt% in isopropanol), indium tin oxide coated PET (surface resistivity $60 \Omega \text{ sq}^{-1}$) and triethylxonium tetrafluoroborate solution (1.0 M in methylene chloride) were purchased from Sigma-Aldrich. Silver nanowires (SLV-NW-90, average diameter: $90 \pm 20 \text{ nm}$, average length: $30 \mu\text{m}$, 10 mg/mL in isopropanol) were obtained from Blue Nano Inc. (Charlotte, NC, USA). TiO_2 nanoparticles solutions were synthesized according to a previous reference.^[58] Elmer's super fast epoxy cement was ordered from Amazon Inc.

General Methods: Absorption and fluorescence spectra were recorded with a Shimadzu UV-3600 spectrophotometer and a PTI fluorescence system, respectively. Infrared spectroscopic measurements were performed with a Bruker Vertex 70 FTIR spectrophotometer. Transmission electron microscopy (TEM) measurements were conducted with a JEOL 2000FX TEM operated at accelerating voltages of 200 kV. The thickness of active layer was measured by Veeco Dektak 150 surface profiler.

Ligand-Exchange Reactions of CdSe NPs: The ligand of the CdSe QDs as received was trioctylphosphine oxide, which was exchanged using a modification of a published procedure.^[35] 0.5 mL of CdSe QDs dispersed in toluene ($\approx 100 \text{ mg mL}^{-1}$) was dried under nitrogen flow and re-dispersed in 10 mL anhydrous hexane. The hexane dispersion was mixed with 10 mL of acetonitrile anhydrous, and was combined with 0.25 mL of dichloromethane solution of Et_3OBF_4 (1 M) at room temperature. The resulting mixture was shaken until the CdSe NPs were transferred from the upper hexane layer to the bottom acetonitrile layer. The NPs were purified by centrifugation (15 000 rpm, 15 min) and re-dispersed in THF (20 mL).

Secondary Ligand-Exchange Reaction of CdSe NPs:^[35] Et_3OBF_4 treated CdSe NPs can be further stabilized by various ligands through a secondary ligand exchange reaction. 0.4 g of 4-mercaptobenzoic acid was added to 20 mL THF solution of CdSe ($\approx 5 \text{ mg mL}^{-1}$) previously modified. The resulting solution was stirred at room temperature overnight. The surface modified NPs were precipitated and purified by centrifugation (15 000 rpm, 5 min), then re-dispersed in cyclohexanone ($\approx 10 \text{ mg mL}^{-1}$).

Device Fabrication and Measurements: Indium tin oxide (ITO)-coated glass substrates ($20 \pm 5 \Omega \text{ sq}^{-1}$) were purchased from Thin Film Devices Inc. The quantum dot light-emitting electrochemical cells were fabricated according to the following procedure: ITO-coated glass was cleaned by ultrasonic treatment for 15 min sequentially in detergent, deionized water, acetone and 2-propanol and then dried under nitrogen flow. After completely drying, ITO-coated glass was treated with UV-ozone for 15 min to improve the wettability of PEDOT:PSS. PEDOT:PSS (Baytron P VP A1 4083) ($\approx 35 \text{ nm}$) was spin-coated onto the ITO substrates and annealed on a hot plate at $150 \text{ }^\circ\text{C}$ for 30 min in air. The substrates were then transferred to glove box. PVK (12.5 mg) and ionic liquid BMIM-PF₆ (2.5 mg) were dissolved in 1 mL QDs solution in cyclohexanone (10 mg mL^{-1}), and the solution was stirred for half hour at room temperature before use. The active layer was spin-coated on top of PEDOT:PSS layer at 1000 rpm for 60 s, yielding a layer thickness of approximately 150–200 nm. Finally, an Al cathode was thermally evaporated following overnight drying under high vacuum (10^{-7} mbar) through a shadow mask with active areas of 6 mm^2 . Devices were encapsulated by epoxy in glove box before testing. Device performance was measured in air using a Keithley 2602 Sourcemeter and a calibrated Ocean Optics USB 4000 UV-vis spectrometer.

Fabrication of Transparent and Flexible Devices: 1) Transparent devices on glass substrates were fabricated using the device structure: Glass/ITO/PEDOT:PSS/QD active layer/AgNW. The procedures prior to deposition of AgNW were the same as those used for the devices with Al as cathode. The AgNW composite electrode was deposited according to published reports.^[56,57] Silver nanowires (2 mg mL^{-1} in isopropanol, 2000 rpm, 60 s) were spin-coated on the active layer. Then a TiO_2 sol-gel solution (0.1 wt% in ethanol, 2000 rpm, 60 s) was spin-coated on top of the silver nanowires and baked at $100 \text{ }^\circ\text{C}$ for 10 s. ITO nanoparticles (10 wt% in isopropanol) were used as conductive fillers and was spin-coated (2000 rpm, for 60 s) onto the fused AgNW to form the composite electrode. 2) Flexible devices were fabricated using the device structure:

PET/ITO/PEDOT:PSS/QD active layer/Al. ITO electrodes on PET were patterned using Scotch tape as a mask followed by etching in dilute hydrochloric acid (HCl). The other procedures were the same as those used for the devices on glass.

Supporting Information

Supporting Information is available from the Wiley Online Library or from the author.

Acknowledgements

Funding for this research was provided by the National Science Foundation through the Center for Hierarchical Manufacturing (CHM, CMMI-1025020) at UMass Amherst. The authors thank the QD Vision Inc. for providing the luminescent quantum dots used in this work.

Received: January 17, 2014

Revised: February 21, 2014

Published online: May 2, 2014

- [1] C. B. Murray, D. J. Norris, M. G. Bawendi, *J. Am. Chem. Soc.* **1993**, *115*, 8706.
- [2] V. L. Colvin, M. C. Schlamp, A. P. Alivisatos, *Nature* **1994**, *370*, 354.
- [3] S. Coe, W.-K. Woo, M. Bawendi, V. Bulovic, *Nature* **2002**, *420*, 800.
- [4] S. Coe-Sullivan, J. S. Steckel, W.-K. Woo, M. G. Bawendi, V. Bulovic, *Adv. Funct. Mater.* **2005**, *15*, 1117.
- [5] J. S. Steckel, P. Snee, S. Coe-Sullivan, J. P. Zimmer, J. E. Halpert, P. Anikeeva, L.-A. Kim, V. Bulovic, M. G. Bawendi, *Angew. Chem., Int. Ed.* **2006**, *45*, 5796.
- [6] J. S. Steckel, J. P. Zimmer, S. Coe-Sullivan, N. E. Stott, V. Bulovic, M. G. Bawendi, *Angew. Chem. Int. Ed.* **2004**, *43*, 2154.
- [7] J. S. Steckel, S. Coe-Sullivan, V. Bulovic, M. G. Bawendi, *Adv. Mater.* **2003**, *15*, 1862.
- [8] X. Peng, M. C. Schlamp, A. V. Kadavanich, A. P. Alivisatos, *J. Am. Chem. Soc.* **1997**, *119*, 7019.
- [9] I. H. Campbell, B. K. Crone, *Appl. Phys. Lett.* **2008**, *92*, 043303.
- [10] Q. Sun, Y. A. Wang, L. S. Li, D. Wang, T. Zhu, J. Xu, C. Yang, Y. Li, *Nat. Photonics* **2007**, *1*, 717.
- [11] B. S. Mashford, M. Stevenson, Z. Popovic, C. Hamilton, Z. Zhou, C. Breen, J. Steckel, V. Bulovic, M. Bawendi, S. Coe-Sullivan, P. T. Kazlas, *Nat. Photonics* **2013**, *7*, 407.
- [12] Q. Pei, G. Yu, C. Zhang, Y. Yang, A. J. Heeger, *Science* **1995**, *269*, 1086.
- [13] Y. Hu, J. Gao, *J. Am. Chem. Soc.* **2011**, *133*, 2227.
- [14] Y. Hu, J. Gao, *J. Am. Chem. Soc.* **2009**, *131*, 18236.
- [15] P. Matyba, K. Maturova, M. Kemerink, N. D. Robinson, L. Edman, *Nat. Mater.* **2009**, *8*, 672.
- [16] J. Fang, P. Matyba, L. Edman, *Adv. Funct. Mater.* **2009**, *19*, 2671.
- [17] J. D. Slinker, J. A. DeFranco, M. J. Jaquith, W. R. Silveira, Y. W. Zhong, J. M. Moran-Mirabal, H. G. Craighead, H. D. Abruna, J. A. Marohn, G. G. Malliaras, *Nat. Mater.* **2007**, *6*, 894.
- [18] S. v. Reenen, P. Matyba, A. Dzwilewski, R. A. J. Janssen, L. Edman, M. Kemerink, *J. Am. Chem. Soc.* **2010**, *132*, 13776.
- [19] M. Lenes, G. Garcia-Belmonte, D. Tordera, A. Pertegás, J. Bisquert, H. J. Bolink, *Adv. Funct. Mater.* **2011**, *21*, 1581.
- [20] J. C. deMello, N. Tessler, S. C. Graham, R. H. Friend, *Phys. Rev. B* **1998**, *57*, 12951.
- [21] J. deMello, *Phys. Rev. B* **2002**, *66*, 235210.
- [22] Y. Yang, Q. Pei, *Appl. Phys. Lett.* **1996**, *68*, 2708.
- [23] M. Sun, C. Zhong, F. Li, Y. Cao, Q. Pei, *Macromolecules* **2010**, *43*, 1714.

- [24] S. Tang, J. Pan, H. A. Buchholz, L. Edman, *J. Am. Chem. Soc.* **2013**, *135*, 3647.
- [25] Y. Hu, Y. Zhang, J. Gao, *Adv. Mater.* **2006**, *18*, 2880.
- [26] S. Tang, J. Pan, H. Buchholz, L. Edman, *ACS Appl. Mat. Interfaces* **2011**, *3*, 3384.
- [27] J. D. Slinker, A. A. Gorodetsky, M. S. Lowry, J. Wang, S. Parker, R. Rohl, S. Bernhard, G. G. Malliaras, *J. Am. Chem. Soc.* **2004**, *126*, 2763.
- [28] A. Paul, R. A. Bartels, R. Tobey, H. Green, S. Weiman, I. P. Christov, M. M. Murnane, H. C. Kapteyn, S. Backus, *Nature* **2003**, *421*, 51.
- [29] H. J. Bolink, L. Cappelli, E. Coronado, M. Grätzel, E. Ortí, R. D. Costa, P. M. Viruela, M. K. Nazeeruddin, *J. Am. Chem. Soc.* **2006**, *128*, 14786.
- [30] D. Tordera, A. Pertegás, N. M. Shavaleev, R. Scopelliti, E. Ortí, H. J. Bolink, E. Baranoff, M. Grätzel, M. K. Nazeeruddin, *J. Mater. Chem.* **2012**, *22*, 19264.
- [31] N. Armaroli, G. Accorsi, M. Holler, O. Moudam, J.-F. Nierengarten, Z. Zhou, R. T. Wegh, R. Welter, *Adv. Mater.* **2006**, *18*, 1313.
- [32] H. J. Bolink, E. Coronado, R. D. Costa, E. Ortí, M. Sessolo, S. Graber, K. Doyle, M. Neuburger, C. E. Housecroft, E. C. Constable, *Adv. Mater.* **2008**, *20*, 3910.
- [33] L. He, L. Duan, J. Qiao, R. Wang, P. Wei, L. Wang, Y. Qiu, *Adv. Funct. Mater.* **2008**, *18*, 2123.
- [34] A. J. Norell Bader, A. A. Ilkevich, I. V. Kosilkin, J. M. Leger, *Nano Lett.* **2011**, *11*, 461.
- [35] A. Dong, X. Ye, J. Chen, Y. Kang, T. Gordon, J. M. Kikkawa, C. B. Murray, *J. Am. Chem. Soc.* **2011**, *133*, 998.
- [36] H. D. Lutz, J. Himmrich, M. Schmidt, *J. Alloys Compd.* **1996**, *241*, 1.
- [37] I.-S. Liu, H.-H. Lo, C.-T. Chien, Y.-Y. Lin, C.-W. Chen, Y.-F. Chen, W.-F. Su, S.-C. Liou, *J. Mater. Chem.* **2008**, *18*, 675.
- [38] S. F. Wuister, C. d. M. Donegá, A. Meijerink, *J. Phys. Chem. B* **2004**, *108*, 17393.
- [39] Y. Wang, N. Herron, *Chem. Phys. Lett.* **1992**, *200*, 71.
- [40] B. O. Dabbousi, M. G. Bawendi, O. Onitsuka, M. F. Rubner, *Appl. Phys. Lett.* **1995**, *66*, 1316.
- [41] B. S. Mashford, M. Stevenson, Z. Popovic, C. Hamilton, Z. Zhou, C. Breen, J. Steckel, V. Bulovic, M. Bawendi, S. Coe-Sullivan, P. T. Kazlas, *Nat. Photonics* **2013**, *7*, 407.
- [42] C. R. Kagan, C. B. Murray, M. G. Bawendi, *Phys. Rev. B* **1996**, *54*, 8633.
- [43] J.-M. Caruge, J. E. Halpert, V. Bulovic, M. G. Bawendi, *Nano Lett.* **2006**, *6*, 2991.
- [44] Y. Q. Li, A. Rizzo, R. Cingolani, G. Gigli, *Adv. Mater.* **2006**, *18*, 2545.
- [45] P. O. Anikeeva, J. E. Halpert, M. G. Bawendi, V. Bulovic, *Nano Lett.* **2007**, *7*, 2196.
- [46] C. R. Kagan, C. B. Murray, M. Nirmal, M. G. Bawendi, *Phys. Rev. Lett.* **1996**, *76*, 1517.
- [47] S. Crooker, J. Hollingsworth, S. Tretiak, V. Klimov, *Phys. Rev. Lett.* **2002**, *89*, 186802.
- [48] V. Bulović, G. Gu, P. E. Burrows, S. R. Forrest, M. E. Thompson, *Nature* **1996**, *380*, 29.
- [49] V. Wood, M. J. Panzer, J.-M. Caruge, J. E. Halpert, M. G. Bawendi, V. Bulović, *Nano Lett.* **2010**, *10*, 24.
- [50] G. Parthasarathy, C. Adachi, P. E. Burrows, S. R. Forrest, *Appl. Phys. Lett.* **2000**, *76*, 2128.
- [51] T. Ouisse, M. Armand, Y. Kervella, O. Stephan, *Appl. Phys. Lett.* **2002**, *81*, 3131.
- [52] L. Hu, D. S. Hecht, G. Grüner, *Nano Lett.* **2004**, *4*, 2513.
- [53] A. K. Geim, K. S. Novoselov, *Nat. Mater.* **2007**, *6*, 183.
- [54] M.-G. Kang, M.-S. Kim, J. Kim, L. J. Guo, *Adv. Mater.* **2008**, *20*, 4408.
- [55] R. Zhu, A. Kumar, Y. Yang, *Adv. Mater.* **2011**, *23*, 4193.
- [56] R. Zhu, C.-H. Chung, K. C. Cha, W. Yang, Y. B. Zheng, H. Zhou, T.-B. Song, C.-C. Chen, P. S. Weiss, G. Li, Y. Yang, *ACS Nano* **2011**, *5*, 9877.
- [57] C.-C. Chen, L. Dou, R. Zhu, C.-H. Chung, T.-B. Song, Y. B. Zheng, S. Hawks, G. Li, P. S. Weiss, Y. Yang, *ACS Nano* **2012**, *6*, 7185.
- [58] J. Wang, J. Polleux, J. Lim, B. Dunn, *J. Phys. Chem. C* **2007**, *111*, 14925.